SUPPLEMENTARY FIGURES

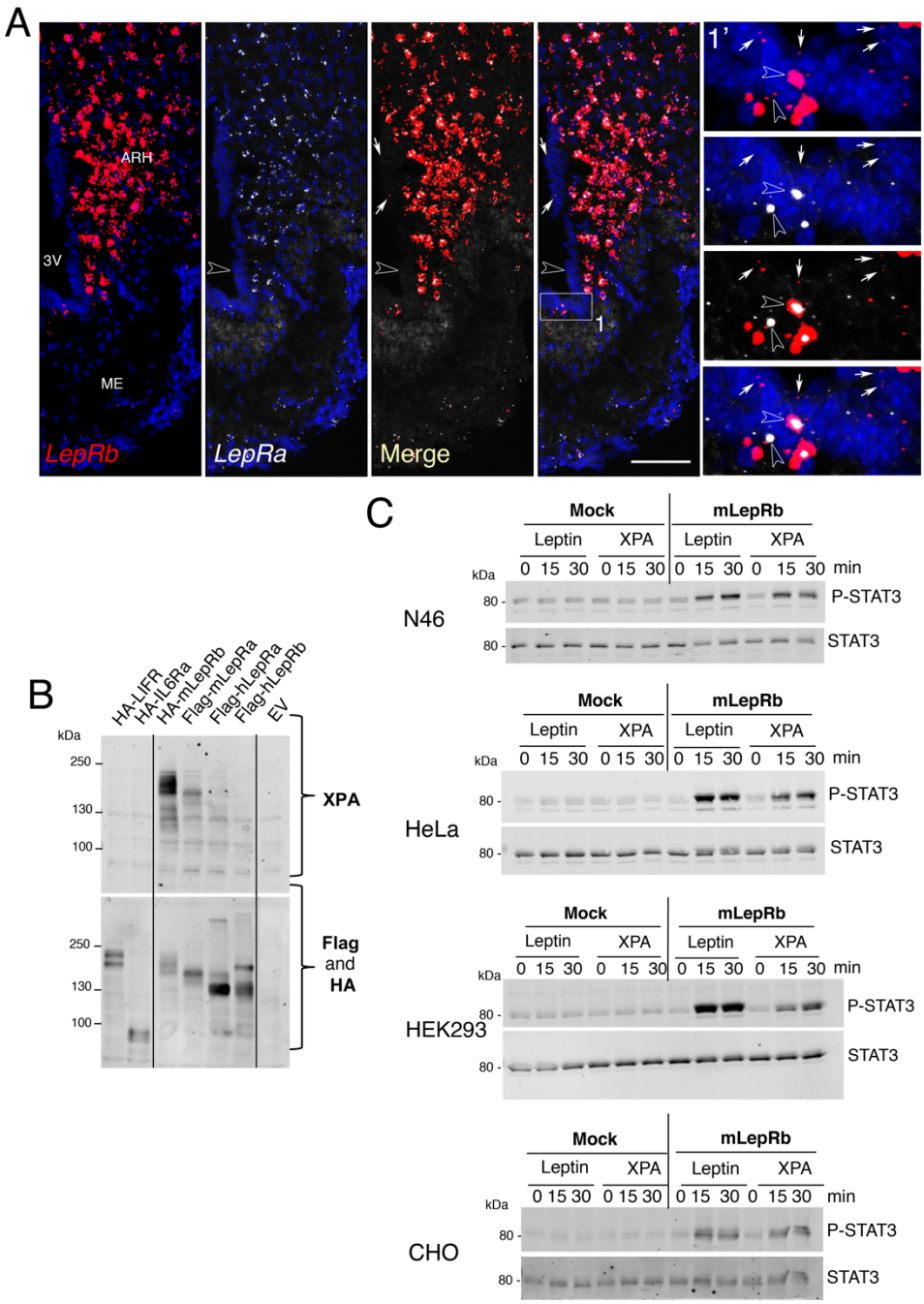

Supplementary Figure 1. *LepRa* and *LepRb* transcript expression in the median eminence and arcuate nucleus of the hypothalamus and characterization of the XPA antibody against LepR.

(**A**) Representative photomicrograph of *in situ* hybridation of LepR long form (LepRb, in red) and short form (LepRa, in white) using RNAscpe technology on fresh-frozen brain section in the median eminence of a $LepR^{loxP/loxP}$ mouse (n=3 mice). Insets magnified at right to show the different types of labeling. Arrows show red dots corresponding to the LepRb transcript; empty arrowheads show cells expressing both red and white dots corresponding to LepRb and LepRa transcripts, respectively. Scale bar: 200 µm (50 µm in insets).

(**B**) Representative Western Blot detection of XPA in cells expressing different cytokine receptors including mouse and human LepRs out of at least 2 independent experiments.

(**C**) Comparison of STAT3 phosphorylation in multiple cell lines stably expressing mouse LepRb and mock controls after stimulation with 50 nM leptin or 100 nM XPA for 5, 15 or 30 minutes out of at least 2 independent experiments.

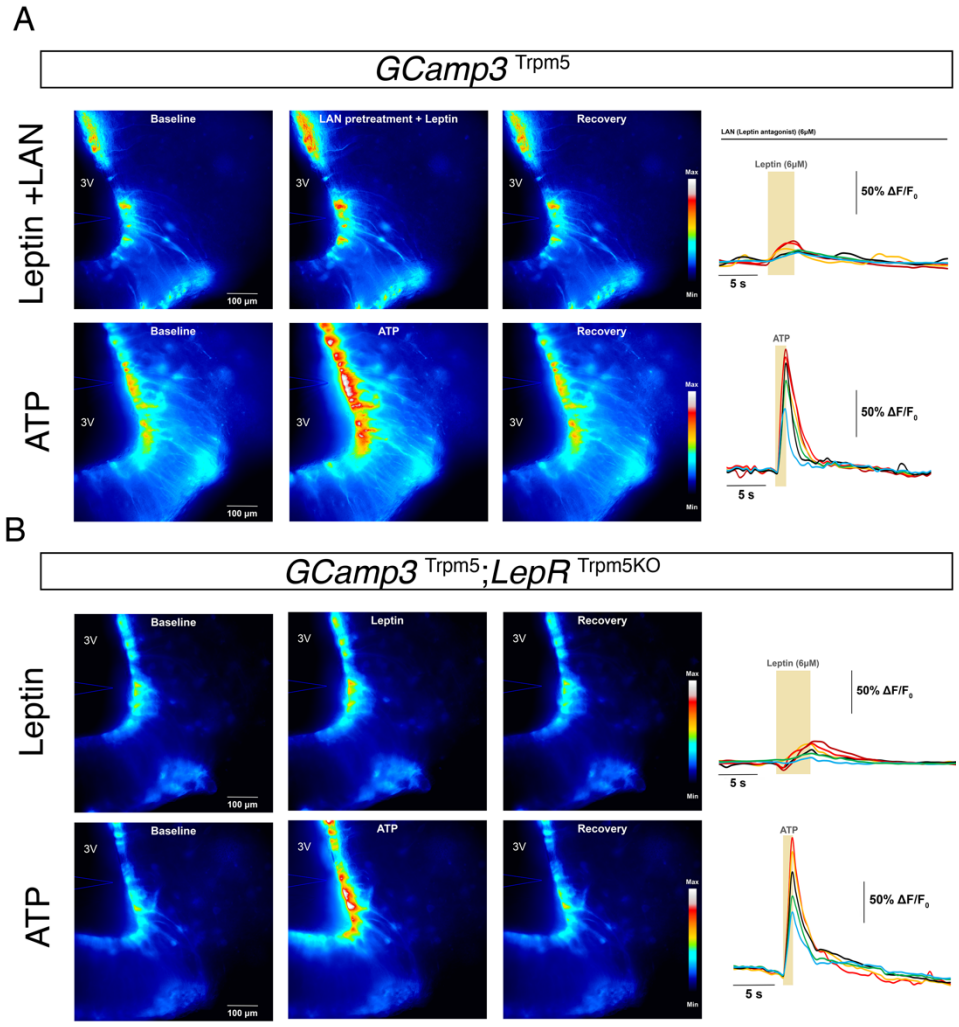

Supplementary Figure 2. Calcium waves in tanycytes in response to local puffs of leptin and ATP in living brain slices from *GCamp3*^{Trpm5} and *GCamp3*^{Trpm5};*LepR*^{Trpm5KO} mice.

(**A**) Representative changes in intracellular calcium concentrations in tanycytes in living brain slices from *GCamp3*^{Trpm5} mice upon puffs of leptin (6µM) after bath-application of LAN (6µM, upper panels) and of ATP (10mM, lower panels).

(**B**) Representative changes in intracellular calcium concentrations in tanycytes in living brain slices from *GCamp3*^{Trpm5};*LepR3*^{Trpm5} mice upon puffs of leptin (6µM, upper panels) and ATP (10mM, lower panels).

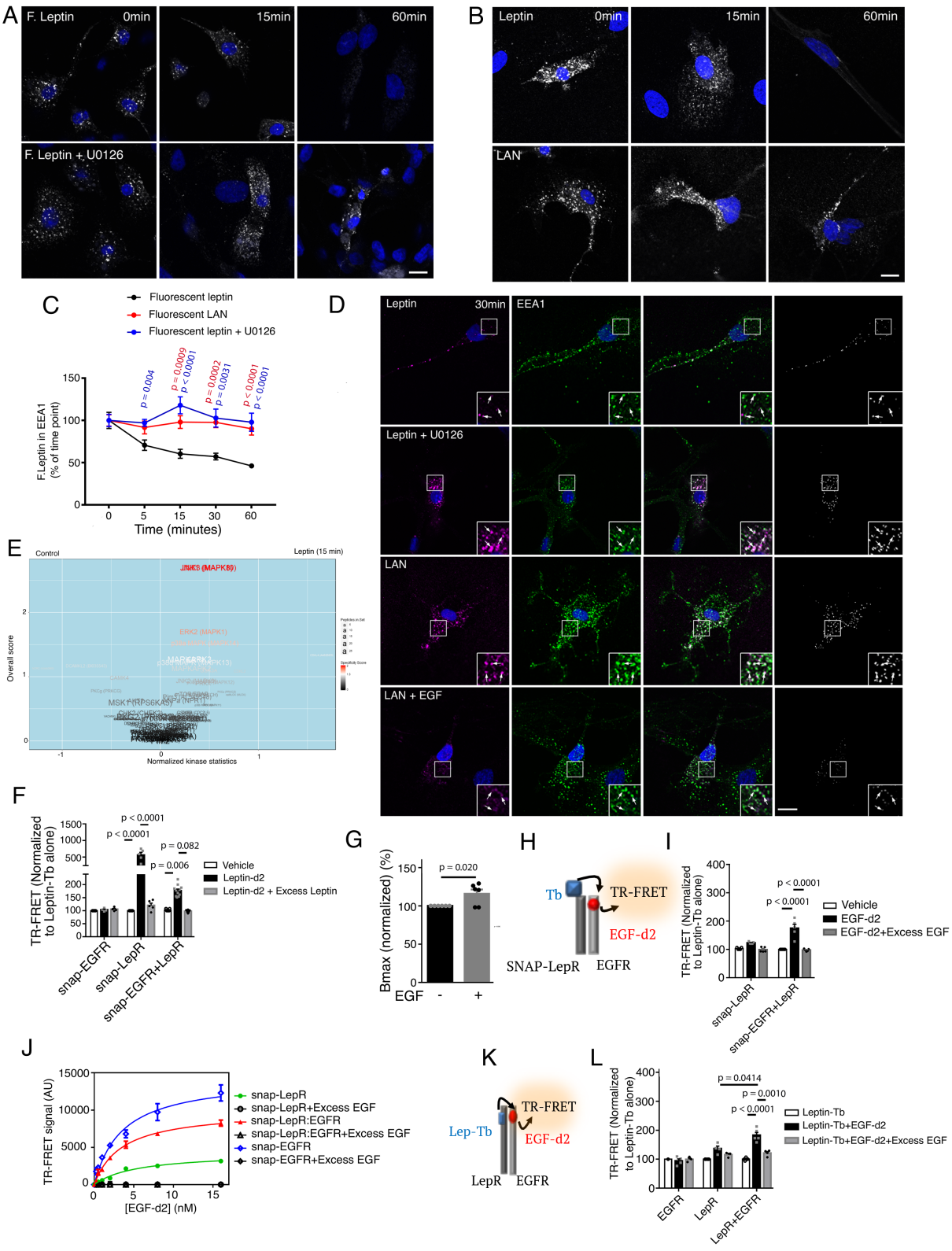

Supplementary Figure 3. Involvement of EFGR and MAPKs in release of internalized leptin from tanycytic early endosomes

(**A**) Kinetics of leptin release by tanycytes. Representative confocal images of tanycytes subjected to a leptin pulse (125 nM) for 15 min (before the 0 min time point) and chased for 15 or 60 min in the absence or presence of the MEK1/2 inhibitor (U0126, 10 µM). Experiments were repeated in at least 2 independent primary cultures of tanycytes. Scale bar: 10 µm

(**B**) Kinetics of LAN release by tanycytes. Representative confocal images for tanycytes subjected to a fluorescent LAN pulse (125 nM) for 15 min (before the 0 min time point) and chased for 15 or 60 min. Experiments were repeated in at least 2 independent primary cultures of tanycytes. Scale bar: 10 µm

(**C**) Graph representing amounts of fluorescent leptin or LAN in cells treated or not with U0126 during the chase experiment (as a % of values at the 0 min time point). Mann-Whitney test. n = 11-36 cells per group from at least 2 independent primary cultures. Values indicate means ± SEM.

(**D**) MAPK signaling is required for leptin to exit early endosomes. Representative confocal images for tanycytes subjected to a fluorescent leptin or LAN pulse for 15 min and chased for 30 min in the absence or presence of U0126 (leptin) or EGF (LAN). Cells were labeled for EEA1 (green). Colocalized pixels are shown on the right panel and arrows in inset point to examples of colocalization. Experiments were repeated in at least 2 independent primary cultures of tanycytes. Scale bar: 10 µm.

(**E**) Volcano plot showing differences in peptide phosphorylation between primary cultures of tanycytes treated with leptin (1 µg/ml in PBS pH 8.0) or vehicle (PBS pH 8.0) for 15 min (n=4 per group). Upstream kinases were identified using the Human Protein Reference Database.

(**F**) The TR-FRET signal generated upon the close proximity of leptin-d2 (1nM) to fluorescent SNAP-EGFR is observed with the LepR:SNAP-EGFR complex but not with fluorescent SNAP-EGFR expressed alone. Two-way ANOVA with Tukey multiple comparison test was applied. n = 4-11 wells per condition from at least 2 independent experiments. Values indicate means ± SEM.

(**G**) Increased Bmax values under conditions of co-stimulation with leptin-d2 +EGF. Two-sided unpaired Student's t-test. n=6 wells per condition from at least 2 independent experiments. Values indicate means ± SEM.

(**H**) Schematic diagram of the TR-FRET-based assay for EGF-d2 binding to the SNAP-LepR:EGFR complex.

(**I**) The TR-FRET signal due to the close proximity of EGF-d2 (1nM) to fluorescent SNAP-LepR, associated with endogenously expressed EGFR, is increased with the ectopic expression of EGFR, favoring the formation of the SNAP-LepR:EGFR complex. Two-way ANOVA with Tukey multiple comparison test was applied. n=5 wells per condition from at least 2 independent experiments. Values indicate means ± SEM. (**J**) Saturation of binding of EGF-d2 to SNAP-LepRb- or (LepRb + EGFR)-expressing cells yielded a K_D =3.90 [2.09-5.71] nM and K_D =2.08 [1.63-2.53] nM, respectively. These mean K_D values are comparable to EGF-d2 binding to SNAP-EGFR (K_D =3.21 [2.40-3.69] nM). Data are presented as means ± SD; n = 3 well replicates of 1 representative experiment out of 3 independent experiments. The mean dissociation constant was determined from the average of the K_D values extracted from a fitting analysis of the saturation curve of 3 independent experiments with non-linear regression “one-site specific binding equation” (GraphPad).

(**K-L**) The TR-FRET signal is detected only when LepR and EGFR are co-expressed in cells allowing the proximity of fluorescent leptin-Tb (1nM) with fluorescent EGF-d2 (1nM), with both ligands binding specifically to their cognate receptors within the LepR:EGFR complex. By competing with EGF-d2, an excess of unlabeled EGF (200nM) drastically abrogated the TR-FRET signal. Two-way ANOVA with Tukey multiple comparison test was applied. Values indicate means ± SEM. Each dot represents a well.

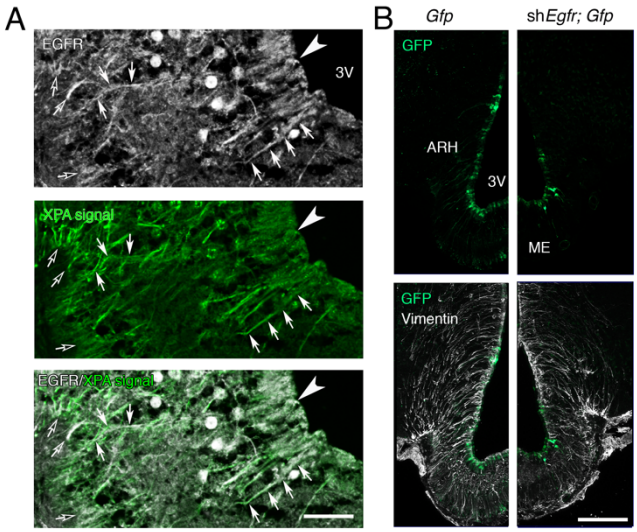

Supplementary Figure 4. EGFR and sh*Egfr* expression in tanycytes of the median eminence.

(**A**) Representative photomicrograph of EGFR immunofluorescence (in white) colocalized with XPA (in green). Colocalized areas are indicated by white arrows. Experiments were performed in 2 mice. Scale bar: 30 µm.

(**B**) Representative photomicrograph showing endogenous GFP and vimentin 16 weeks after *AAV1/2 Dio2::GFP* (left panel) and *AAV(1+2)-GFP-U6-m-EGFR-shRNA* (right panel) infusion into the lateral ventricle. Experiments were performed in 3 mice per group. Scale bar: 200 µm.

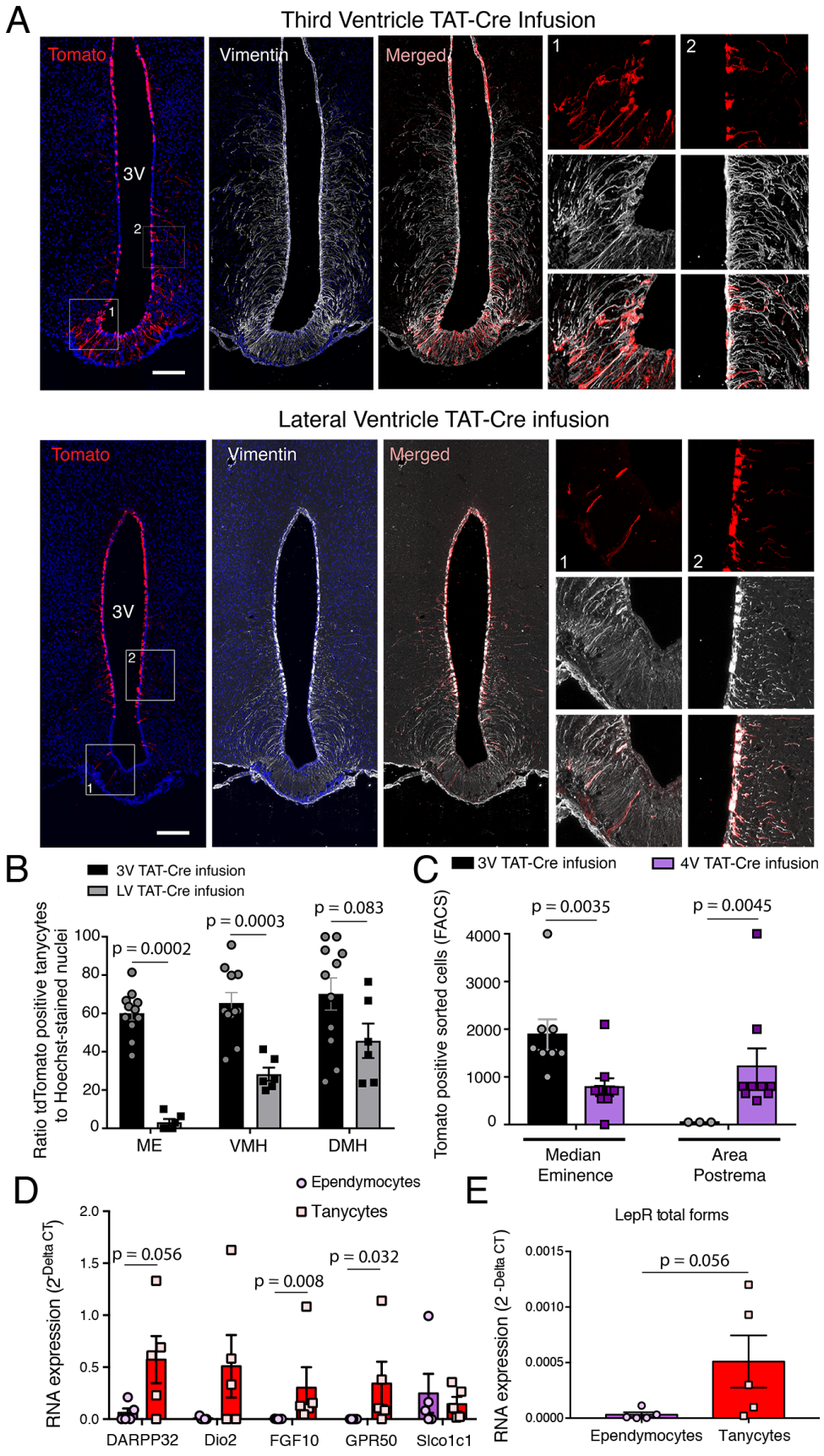

Supplementary Figure 5: Comparative efficiency of TAT-Cre injection sites on gene recombination in median eminence tanycytes, which show enriched LepR expression when compared to ciliated ependymocytes.

(**A**) Representative photomicrographs of endogenous tdTomato (red) and Vimentin (white) in the median eminence and walls of third ventricle after TAT-Cre infusion into the third ventricle (**top row**) or lateral ventricle (**bottom row**) illustrating quantifications in panel **B**. Insets magnified at right to show the cell shape and the precise colocalization of vimentin and tdTomato labeling. Scale bar: 200µm.

(**B**) Graph representing the ratio of tdTomato-positive tanycytes to Hoechst-stained nuclei at different levels of the third ventricle after TAT-Cre infusion into the lateral ventricle (LV) and the third ventricle (3V). Two-sided unpaired Student's t-test. Values indicate means ± SEM. Each dot represents a mouse.

(**C**) Graph representing the number of tdTomato-positive FACS-sorted cells from the median eminence (black) and area postrema (purple) after TAT-Cre injection into the third (black bars) or fourth ventricle (magenta bars). Two-sided unpaired Student's t-test. Values indicate means ± SEM. Each dot represents a mouse.

(**D**) mRNA expression levels of different tanycytic markers (DARPP32, Dio2, FGF10, GPR50) and Slco1c1 in tdTomato-positive cells obtained from the microdissection of the ventral part of the ventricular wall, at the level of the median eminence (in red; tanycytes) and tdTomato-positive cells obtained from the microdissection of the dorsal part of the ventricular wall (in purple; ependymocytes). Mann-Whitney U test. Values indicate means ± SEM. Each dot represents a mouse.

(**E**) mRNA expression of LepR (all forms) in the previous two sorted populations. Mann-Whitney U test. Values indicate means ± SEM. Each dot represents a mouse.

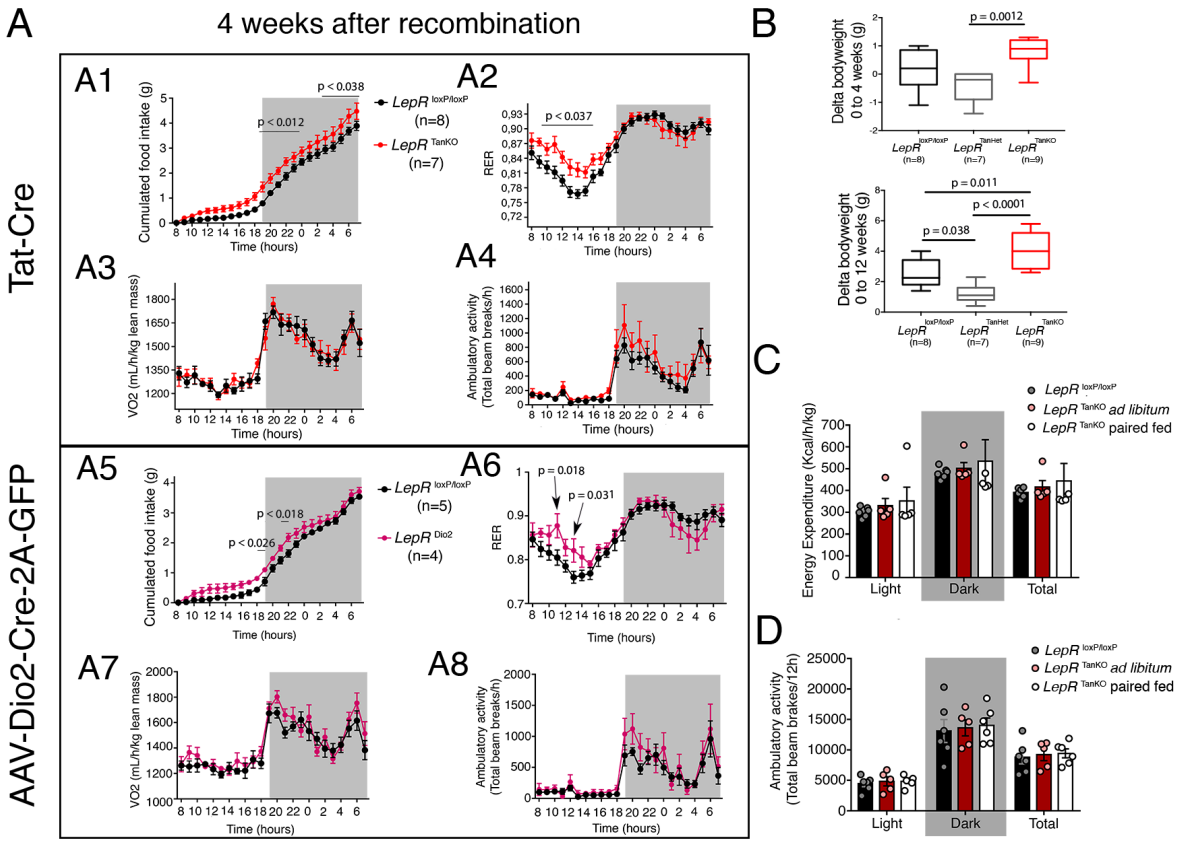

Supplementary Figure 6. Metabolic phenotyping of mice selectively knocked out for the LepR in tanycytes using TAT-Cre and Dio2-driven gene recombination and viral approaches.

(**A**) Four weeks after effective recombination, TAT-Cre (**A1-A4**) and AAV-Dio2-iCre-2A-GFP viral infusion (**A5-A8**) induce the same phenotype in *LepR*$^{loxP/loxP}$ mice with respect to basal metabolism. Two-day basal food intake (**A1** and **A5**), respiratory energy ratio (RER, **A2** and **A6**), oxygen consumption (**A3** and **A7**) and locomotor activity (**A4** and **A8**) monitored in *LepR*^{TanKO} mice 4 weeks after Cre infusion/expression and in control littermates. Two-way ANOVA with uncorrelated Fisher's LSD test. Values indicate means ± SEM. n indicates the number of mice.

(**B**) Delta bodyweight 4 and 12 weeks after TAT-Cre injection in *LepR*^{TanHet} and *LepR*^{TanKO} mice, or vehicle injection in *LepR*$^{loxP/loxP}$ littermates. One-way ANOVA with Tukey's correction. Values in Box-and-whisker plots indicate the minimum, the maximum, the sample median, and the first and third quartiles. n = 7 to 9 mice per group.

(**C-D**) Energy expenditure (**C**) and locomotor activity (**D**) during the pair-fed experiment in *LepR*$^{loxP/loxP}$ and *LepR*^{TanKO} mice, 12 weeks after TAT-Cre infusion. Values indicate means ± SEM. Each dot represents a mouse.

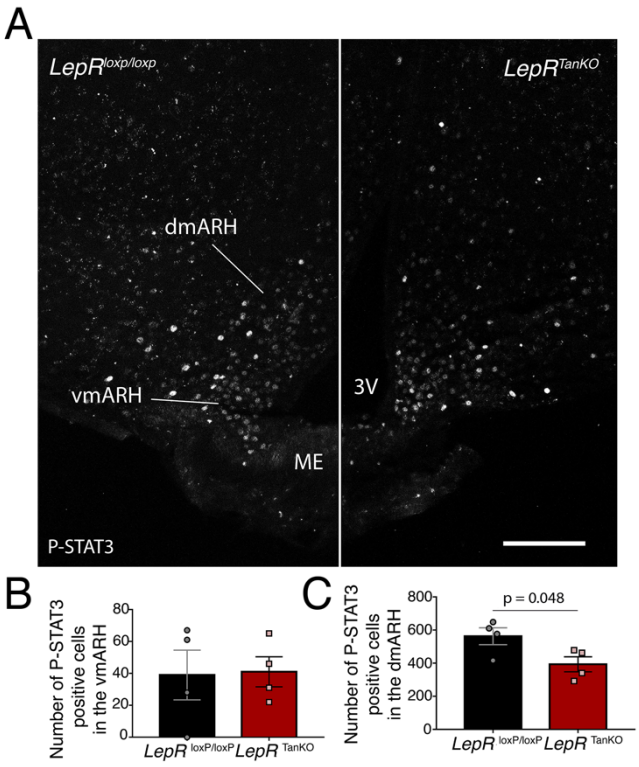

Supplementary Figure 7. Basal P-STAT3 expression in the arcuate nucleus of the hypothalamus of wild type and mutant mice.

(**A-C**) Representative photomicrograph (**A**) and quantification of basal pSTAT3 immunofluorescence in the ventromedial (vm) (**B)** and dorsomedial (dm) arcuate nucleus (ARH) (**C**). Scale bar: 200µm. Unpaired Student's t-test. *: $p<0.05$ *LepR*$^{loxP/loxP}$ vs. *LepR*$^{TanKO.}$ Values indicate means ± SEM. Each dot represents a mouse.

SUPPLEMENTARY TABLES

Gene	Probe ID
DARPP32	Ppp1r1b_Mm00454892_m1
LEPR short form	LepR_Mm1265583_m1
LEPR long form	LepR_Mm01262070_m1
NPY	NPY-Mm03048253_m1
MECA32	Plvap-Mm00453379_m1
POMC	POMC-Mm00435874_m1
AgRP	AgRP-Mm00475829_g1
CART	CARTPT-Mm04210469_m1
Socs3	Socs3-Mm00545913_s1
Ptp1b	Ptp1b-Mm00448427_m1
DIO2	Dio2-Mm00515664_m1
FGF10	Fgf10-Mm00433275_m1
GPR50	Gpr50-Mm00439147_m1
SLCO1C1	Slco1c1-Mm00451845_m1
r18S	18S-Hs99999901_s1
ACTB	Actb-Mm00607939_s1

Table S1. List of TaqMan primers

Gene	Sense Primer	Antisense Primer
Cyclophiline	ATGGCACTGGCGGCAGGTCC	TTGCCATTCCTGGACCCAAA
Glut2	AACCGGGATGATTGGCATGT	GGCGAATTTATCCAGCAGCA
Gck	GCTCAGTGAACCCCGGTCAGC	TGTGCGCAGCTGCTCTGAGG
Kcnj11	CACAAGCTGGGTTGGGGGCTC	TGCCCCTCAGCTGGGTTCTGC
Glp-1r	GTTTCCTCACGGAAGCGCCA	AAGGAACCTGGGGGCCCATC
Ins1	GCCAAACAGCAAAGTCCAGG	GTTGAAACAATGACCTGCTTGC
Pcsk1	TGATGATCGTGTGACGTGGG	GGCAGAGCTGCAGTCATTCT
Pcsk2	AAAGATGGCGCTGCAACAAG	TTGCCCAGTGTTGAACAGGT
Pdx1	ATTGTGCGGTGACCTCGGGC	GATGCTGGAGGGCTGTGGCG
MafA	TCCGACTGAAACAGAAGCGG	CTCTGGAGCTGGCACTTCTC
Nkx2.2	GTGCAGGGAGTATTGGAGGC	GAAGGGCCAGAGGAGGAGA
Hnf1a	GGTGCGTGTCTACAACTGGT	ACCGTACACCGTGGACCTTA
Ucn3	TGATGCCCACCTACTTCCTG	CTGTGTTGAGGCAGCTGAAG
NeuroD1	CTTGGCCAAGAACTACATCTGG	GGAGTAGGGATGCACCGGGAA
ATF4	ATGGCCGGCTATGGATGAT	CGAAGTCAAACTCTTTCAGATCCATT
Xbp1t	GAGCAGCAAGTGGTGGATTT	CCGTGAGTTTTCTCCCGTAA
Xbp1s	GAGTCCGCAGCAGGTG	GTGTCAGAGTCCATGGGA
ChOP	CTGCCTTTCACCTTGGAGAC	CGTTTCCTGGGGATGAGATA
Ero1b	GGGCCAAGTCATTAAAGGAA	TTTATCGCACCCAACACAGT
PPP1R15a	GAGATTCCTCTAAAAGCTCGG	CAGGGACCTCGACGGCAGC
Pdia4	AGTCAAGGTGGTGGTGGGAAAG	TGGGAGCAAAATAGATGGTAGGG
Edem1	AAGTCTCAGGAGCTCAGAGTCATTAA	CGATCTGGCGCATGTAGATG

Table S2. List of the primers used for real-time qPCR in Figure 6J and 6K

Supplementary Figure 1 uncropped Blots

Figure S1B

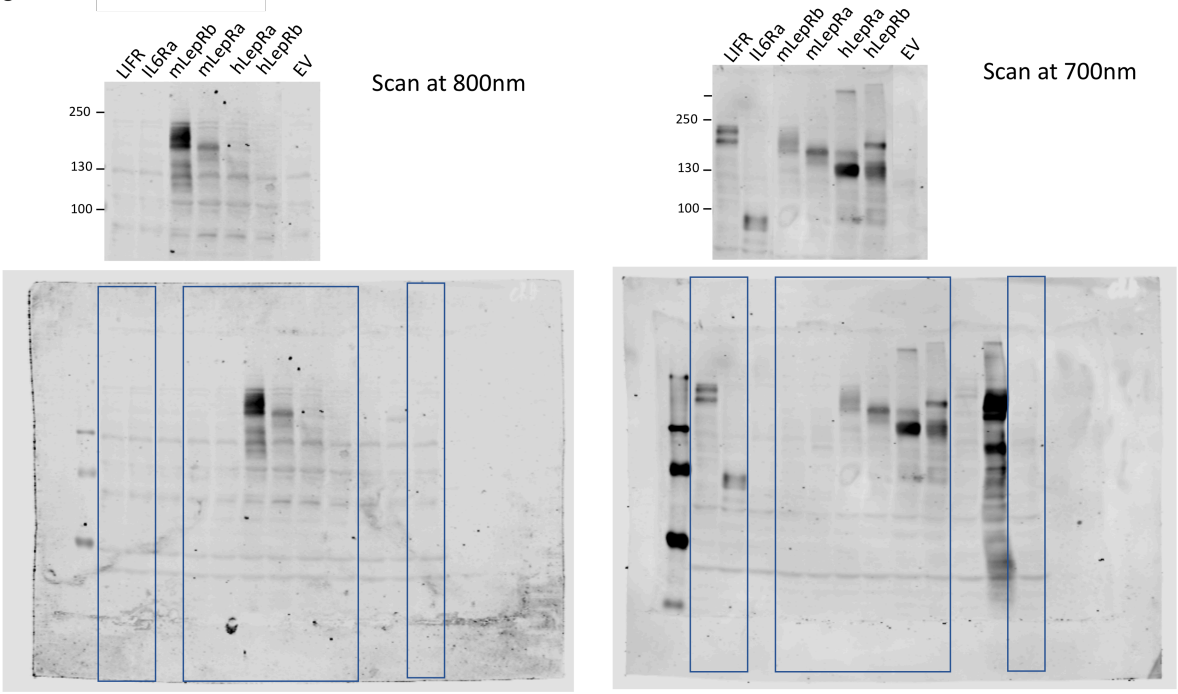

Figure S1C

N46

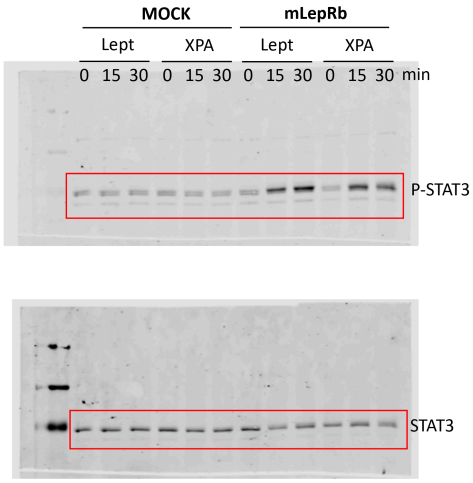

HeLa

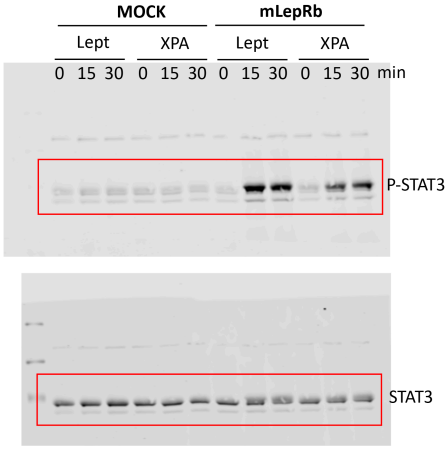

HEK293

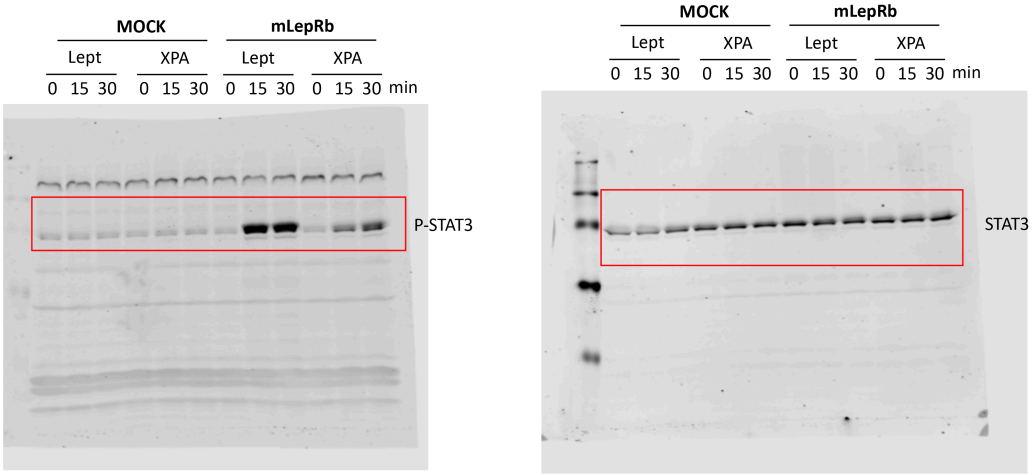
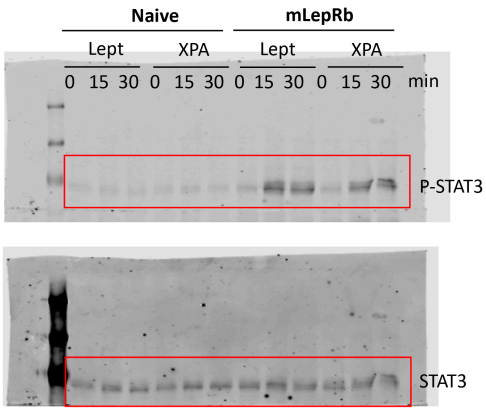
CHO